CORROSION OF ALLOY 800 IN PHWR PRIMARY AND SECONDARY CONDITIONS

A.J.G. Maroto, M.A. Blesa, M. Villegas, A.M. Olmedo, R. Bordoni, M.G. Alvarez, R. Saínz*

ABSTRACT

A hot leg section of a steam generator tubing was removed for destructive examination from one of the steam generators (SG) of the Embalse Nuclear Power Plant. The tube material is Alloy 800 and carbon steel is the tube support plate material. Samples of the deposits were taken at the first tube support plate and at the top, mid-height and bottom of the sludge pile. Transverse sections were taken at several locations along the tube length measuring the oxide thicknesses and studying the morphology of the oxide layer by scanning electron microscopy on the primary and secondary side at each location. Deposit layers on the outer tube surface revealed iron as major component and the presence of calcium, phosphorous, zinc and manganese. The oxide scale thickness at the secondary side in the open area was around 22 to 30 μm.

The oxide thickness grown under isothermal conditions on the corrosion test samples installed in the autoclaves facilities of the primary circuit of the plant was measured and compared with that found on the inner surface of the examined tube section. The oxide thickness of the test samples was around 1-2 μm showing the influence of the deposition of corrosion products from the coolant. Deposition and precipitation of oxide was also found in the actual tube, where the common feature was the irregularity of the oxide layer on the primary side and thicknesses values in the range 4 to 10 μm were measured. The autoclave tests and SG tubing examination permit to compare the influence of materials and of operating (flow rate, isothermal vs non-isothermal) conditions on corrosion and deposition.

Comisión Nacional de Energía Atómica
Avda Libertador 8250, Buenos Aires, 1429, Argentina

*** Central Nuclear Embalse**
Nucleoeléctrica Argentina S.A.

CORROSION OF ALLOY 800 IN PHWR PRIMARY AND SECONDARY CONDITIONS

A.J.G. Maroto, M.A. Blesa, M. Villegas, A.M. Olmedo, R. Bordoni, M.G. Alvarez, R. Saínz

1. INTRODUCTION

The operating experience of nuclear power plants has shown that the unavailability of steam generators (SG) is often related to corrosion, mainly due to tube degradation [1, 2]. Failures are generally originated on the external side of the tubes, usually linked with the existence of deposits since secondary side fouling implies blockage of support plates, accumulation of sludge piles on the tubesheet, concentration of impurities in crevices under deposits and a build-up of scale on the SG tubing itself that affects the heat transfer efficiency. Further to the well known impact of secondary side deposits, primary side fouling of the tubes has also been related to the increase in heat transfer resistance [3].

This work compares the composition, thickness and morphology of the primary side scale found in an actual SG tubing removed from the Embalse Nuclear Power Plant (NPP) with the characteristics of the oxide layer grown under isothermal conditions on the corrosion test samples of SG tubing material installed in the autoclaves facilities of the primary circuit during the routine materials surveillance programme of the plant [4]. The secondary side scale of the tube and samples of the deposits in the sludge pile and the first tube support plate are also characterized.

2. DESCRIPTION OF THE SYSTEM

Embalse NPP is a 648 Mwe CANDU-600 type pressurized heavy water reactor (PHWR). The primary heat transport system (PHTS) has two separate heat transport circuits, each one with two steam generators of the recirculating type with integral preheater. The system is provided with four in-line autoclaves, located out of core in the primary coolant system, that are used to monitor corrosion at outlet and inlet SG conditions (265 and 305°C). The autoclaves are made from carbon steel tube, mounted vertically and provided with stainless steel coupon holders where the specimens are attached. The coolant is lithiated heavy water, $pH_{25°C}$=10.2-10.8, hydrogen content 3-10 cm^3/kg D_2O.

The steam generators have Alloy 800 tubes and trifoil-broached carbon steel tube support plates. Chemical control of the secondary side water is performed using All Volatile Treatment (AVT) with morpholine and hydrazine. Piping is made from carbon steel, the condensers are tubed with Admiralty brass and lake water is used as source of cooling water.

3. EVALUATION OF CORROSION TEST SAMPLES DURING PLANT OPERATION

3.1. Weight-gain during exposure

At the start-up of the Embalse NPP in 1983, samples of Alloy 800 and other structural materials supplied by AECL were installed in the on-line autoclaves. In 1988, coupons of original SG tubing, nuclear grade Alloy 800 provided by the plant, were also inserted.

The inspection of the corrosion samples is routinely programmed every two years, unless the corrosion behaviour of the materials during a specific event has to be monitored. The corrosion coupons are weighed before installation and during each programmed inspection. During the first routine inspection in 1986, the specimens were weighed and optically inspected to check for crud deposits and some test samples were removed to evaluate the oxide formation by ultrasonic cleaning and descaling. Before the second inspection was performed there was a resin ingress to the primary circuit of the plant. On account of this chemical excursion, four inspections were made during 1988, another two during 1989, with a conditioning procedure with hydrazine in-between, and from then on the original time table was resumed [5].

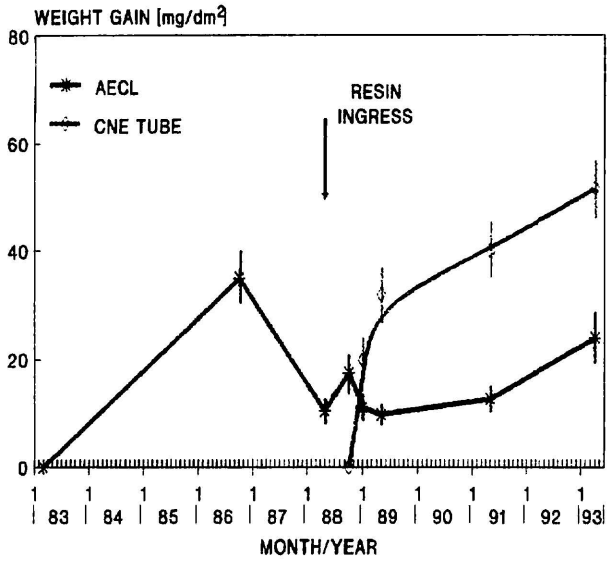


Figure 1: Weight-gain of corrosion test samples in autoclave Y1

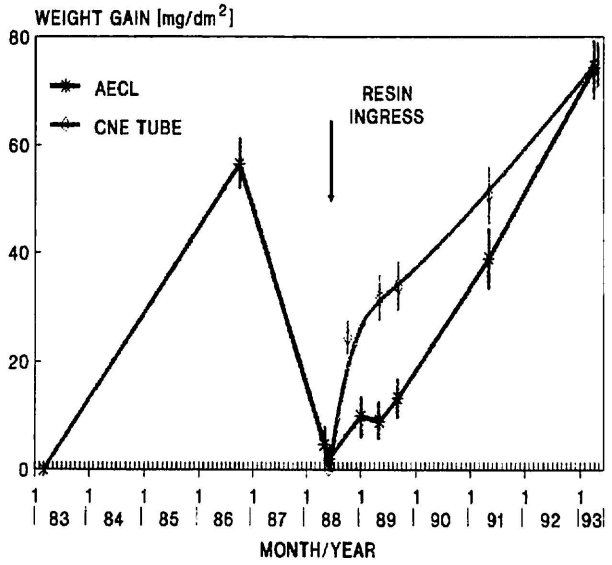


Figure 2: Weight-gain of corrosion test samples in autoclave Y4

Figures 1 and 2 show the weight-gain of the samples in the hot leg autoclaves as a function of the exposure time. Up to 1986, the AECL coupons showed a weight-gain in both autoclaves. In May 1988, the degradation of the mixed resins in the coolant led to a large defilming effect reflected by the weight-loss of the samples.

The following inspections indicated the instability of the corrosion film growing on the AECL coupons, while the plant test samples inserted in 1988 reproduced the corrosion behaviour found up to 1986, i.e. increasing weight-gain with increasing exposure time. After 1989, the weight gain of all test samples showed an increasing trend.

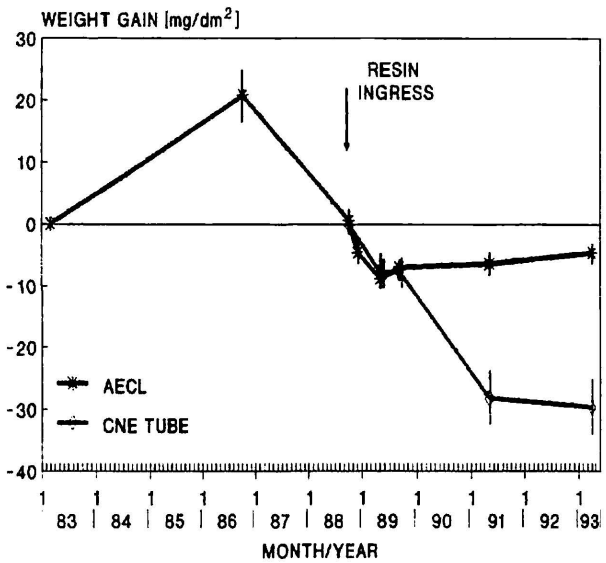


Figure 3: Weight-gain of corrosion test samples in autoclave Y2

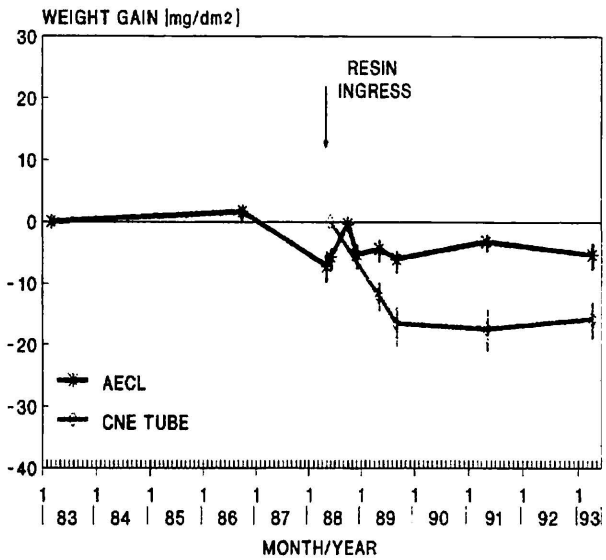


Figure 4: Weight-gain of corrosion test samples in autoclave Y3

Figures 3 and 4 present the data from the test samples in both cold legs. Contrary to the pattern from the hot leg autoclaves, the AECL materials and the plant test samples exhibited a different behaviour. The weight of the AECL materials increased up to 1986 and a weight-loss was observed in May 1988 after the resin degradation. Weight-gains recorded during 1988 and 1989 indicated the lack of stability of the corrosion film but the values stabilized after the conditioning of the plant. The plant test samples introduced in 1988 systematically lost weight during the first 15 months reaching near constancy in weight afterwards.

The increasing weight-gain of the specimens in the hot leg autoclaves indicates that more oxide is accrued on the test sample than that generated by the corrosion process, pointing to the interaction with the corrosion-product saturated coolant, mass transfer and precipitation processes. On the other hand, the weight-loss of the coupons inserted in 1988 in the cold legs corresponds to the dissolution of the outer layer crystals in unsaturated coolant and to continuing corrosion release, partially offset by some thickening of the film. The different behaviour of the samples in the inlet and outlet autoclaves could be related to the differences of the overflowing solution, i.e. system effects, that affect the interaction between dissolved corrosion products and the corroding surface.

3.2. Morphology of the oxide layers

The morphology of the oxide layers was examined by scanning electron microscopy (SEM). The morphology of the oxides grown on the test samples is similar to the typical duplex structure that has been reported for high temperature aqueous corrosion of iron and iron-base alloys [6,7]. The oxide film is generally described as a uniform inner layer that grows into the metal and an outer layer formed by a regular deposit of mostly well-defined octahedral crystals enriched in iron.

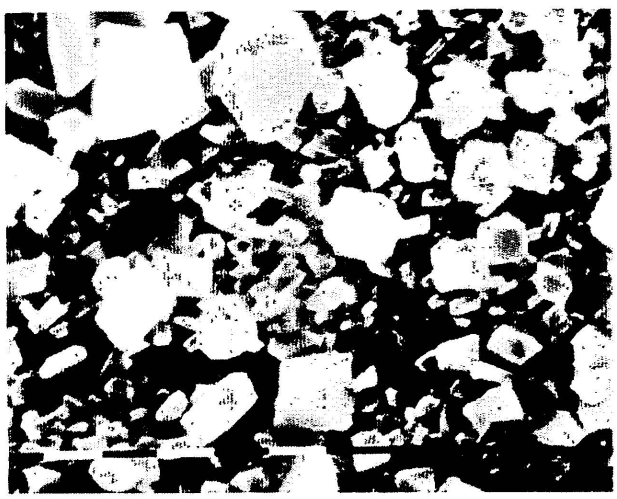


Figure 5: Oxide film grown in primary coolant Line 1 μm

Figure 5 shows the morphology of the oxide layer grown on a test sample from a hot leg autoclave during 1290 days. The surface of the sample was covered by a large number of crystallites that hindered the detection of the inner layer, as was previously reported for long term static autoclave testing [8,9]. The crystallites of larger size, around 2-4 μm, were analyzed by EDS, the major element identified was iron.

The coverage of the surface of the corrosion test samples and the enrichment in iron of the crystallites were similar for all the specimens removed from the autoclaves at the different exposure times.

3.3. Average thickness of the oxide layers

Oxide thicknesses of the different samples were calculated either from corrosion penetration (d_{Me}) or from the weight-loss of the oxidized specimen after chemical descaling (d_{oxid}).

Table I. Average thickness of oxide layers grown in exposures at the Embalse NPP

Sample	Temperature (°C)	Time (days)	d_{Me} (μm)	d_{oxid} (μm)
I-28	305	600	0.61	0.77
I-7	305	1290	0.56	1.65
I-27	305	1290	0.61	1.77
I-49*	265	720	0.68	0.78
I-11	265	695	1.25	0.57
I-30	265	1760	1.50	0.75

* Sample exposed during the 1983-1986 period

Table I presents the results obtained for specimens exposed to the coolant in Embalse's autoclaves. For the specimens from the autoclaves of both hot legs, i.e. inlet SG conditions, d_{oxid} is always larger than d_{Me}. On the other hand, for specimens from the autoclaves located in both cold legs, i.e. outlet SG conditions, d_{oxid} is lower than d_{Me}. An exception to this behaviour was found in the AECL corrosion samples that indicated weight-gain during the period 1983-1986.

The corrosion rate of Alloy 800 was calculated from the metal-loss of the specimens inserted in Embalse's autoclaves by regularly descaling sets of samples from all four autoclaves. Either from the hot or cold legs, the calculated values were in agreement with those reported for Alloy 800 [10], and were not affected by the deposition of corrosion products or by release from the corroding surface.

3.4. Discussion

The experimental results indicate that the test samples at inlet SG conditions gain weight, have a larger oxide thickness than that expected from the corrosion process and the deposition of corrosion products from the coolant leads to the formation of oxide overlayers. On the other hand, at outlet SG conditions, the samples lose weight and show significant corrosion release. These results emphasize the influence on the corrosion of the alloy in high temperature water of the concentration of dissolved corrosion products in the coolant which, in turn, depends on the contribution of other structural materials as carbon steel to the system. At inlet SG conditions, where the coolant is pressumably saturated in corrosion products, precipitation of an iron-rich oxide occurs at the oxide-coolant interface to relieve local supersaturation. Deposition of corrosion products transported by the coolant is also likely to occur. At outlet SG conditions, exposure to unsaturated coolant can lead to the dissolution of the iron-rich outer layer and to continuous corrosion release.

4. EXAMINATION OF A TUBE REMOVED FROM SG N° 4 OF EMBALSE NPP.

Three sections of a hot leg SG tubing were removed for destructive examination from SG N° 4 during a maintenance outage at Embalse NPP after 2750 effective full power days. No leakage of the tube had been detected during service operation. The three sections spanned the tube sheet, the sludge pile, the first tube support plate and the open area between the first and the second tube support plates. Transverse sections were taken at several locations along the tube and the primary and secondary oxide thicknesses were measured from SEM micrographs. Measurements at each transverse section were performed at 15°-20° intervals and an average value of the oxide thickness was obtained. The morphology and composition of both the internal and external oxide layers were studied by SEM/EDS and concentration profiles of the elements throughout the thickness of the scale were obtained at different locations.

4.1. Primary Side

Along the length of the tube, the common feature was the irregularity of the oxide layer. As an example of the typical pattern observed by SEM in all the locations examined, Figure 6 shows a cross-section from the open area just below the second tube support plate. The majority of the film was due to the growth of crystals by precipitation from the coolant. The thin layer detected at the oxide/metal interface is due to the corrosion process of the base material, the rest of the film corresponds to the precipitation process.

At different locations, deposition of corrosion products was also found. Figure 7 shows a cross-section of a sample located in the open area above the sludge pile. Crystals of around 4 μm were observed within an array of smaller size crystals and the thickness of the film was around 10 μm.

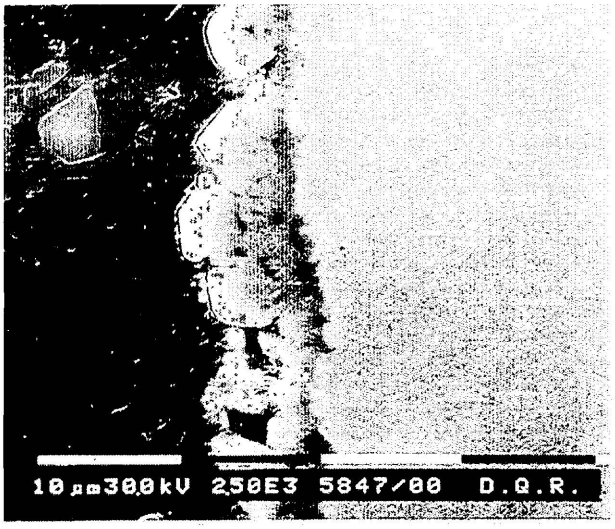


Figure 6: Growth of crystals by precipitation from the primary coolant.



Figure 7: Deposition of corrosion products from the primary coolant.

The oxide film on the inner tube surface contains mainly iron. A significant increase of the iron concentration, as detected by EDS, was found in going from the oxide/metal interface to the oxide/coolant interface associated with the precipitation and deposition of corrosion products from the coolant. Chromium and nickel were present in the inner 4 -5 μm of the film, starting at the metal/oxide interface with values close to those of the alloy material up to a thickness of around 2 μm. From then on, their relative concentration decreased when approaching the middle section of the scale. The EDS analysis were performed on crystals of around 8-10 μm.

The presence of an oxide layer formed by iron, chromium and nickel at this interface is a consequence of the interaction of the alloy surface with the primary coolant medium that gives rise to the growth of a protective layer constituted by chromium and/or nickel ferrites. The growth of these films has been reported [8] in high temperature laboratory tests simulating primary conditions as well as in Alloy 800 tubes, pulled out from operating steam generators of different nuclear power plants, where the thickness of the film was about 4 μm and the outer part of the primary side scale was formed by chromium and/or nickel ferrites [11]. These results correspond to plants built with stainless steel piping, the iron enrichment in the outer part of the primary side scale of the Embalse tube can be attributed to the corrosion products from the carbon steel feed-train piping.

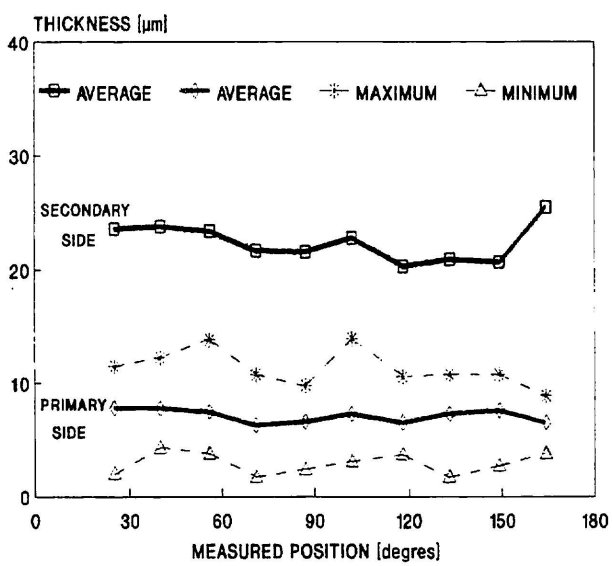


Figure 8: Primary and secondary oxide thicknesses below the second TSP

The average values of the oxide thickness measured at different locations were in the range 4 to 10 μm. Figure 8 presents maximum, minimum and average values of the oxide thickness at the open area just below the second tube support plate, the corresponding morphology was shown in Figure 6. At this location, the average value was 7.1 μm.

The above observations show that the thickness and morphology of the oxide layer inside the tube resemble those of the hot leg corrosion test samples in spite of the influence that the flow rate and the heat exchange through the tube wall may have on the formation of the film, stressing thus the relevance of the concentration of corrosion products in the coolant.

4.2. Secondary side

When comparing the scale formed on the outer surface of the tube with that from the primary side, several distinctions were found: the external oxide is more porous, exhibits at some locations a layered structure and the layer created by the corrosion process of the base metal is not clearly detected at the oxide/metal interface. The thickness of the oxide scale in the open area was around 22 to 30 μm, as is shown in Figure 8, but a thickness of about 100 μm was found immediately over the section covered by the sludge pile. It was only in a section of the tube where no contact with the secondary coolant takes place, such as the region of tube-tube sheet intersection, that the external oxide exhibits the same characteristics and thickness values than those observed on the inner surface of the tube.

SEM/EDS analysis of cross-sections at different locations of the tube identified iron as major component of the deposits but in-depth analysis detected the presence of calcium, phosphorous, zinc, silicon and manganese. The concentration profiles of the elements in the deposits had similar characteristics at all the locations corresponding to the open area. For all cross-sections examined, zinc was detected through-out the thickness of the scale while calcium appeared in localized zones. Whenever calcium was found, it was located near the scale/alloy interface, in the inner 5-10 μm of the film As an example, Figure 9 presents the concentration profiles of these elements in a location above the first tube support plate, the corresponding cross section is shown in Figure 10. A common observation is that an increase in the calcium concentration is always related to a marked decrease in the iron concentration. Calcium predominates in the dark areas of Figure 10 while iron predominates in the light ones. The distribution of phosphorous closely follows that of calcium while zinc, although mostly concentrated near the scale/alloy interface, is relatively shifted beyond calcium. Traces of manganese are evenly distributed across the deposits.

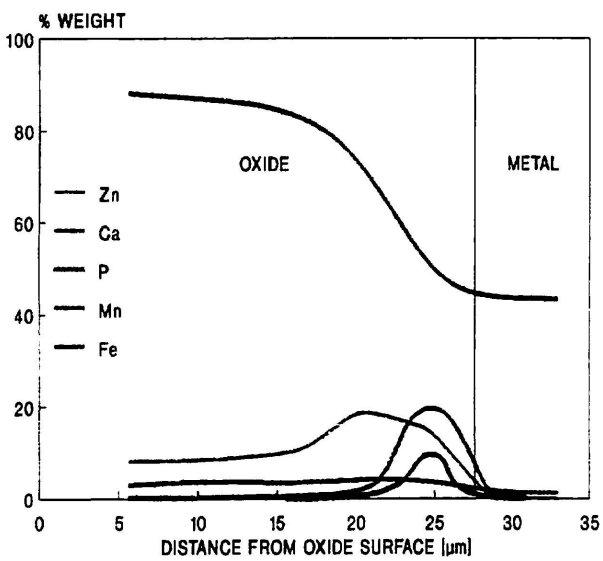


Figure 9: Concentration profiles across the secondary oxide scale.

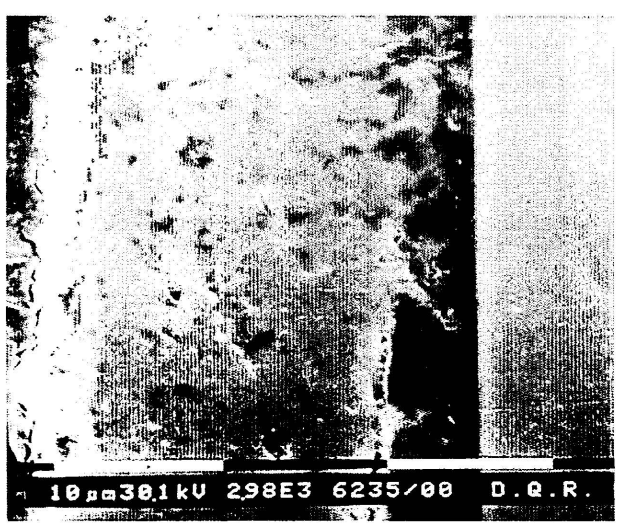


Figure 10: Cross section of the secondary oxide scale.

On the other hand, the concentration profiles obtained at locations immediately over the section covered by the sludge pile showed that although in the 100 μm-thick oxide the same elements were present, the distribution of these elements through-out the thickness of the deposit changes when EDS analysis across the scale is performed at different rotating angles from the same axial position. An optical micrograph at this location shows clearly a layered structure, see Figure 11, and the concentration profiles at two different zones of this oxide scale presented in Figures 12 and 13 indicate the heterogenous composition of the deposit. The concentration of calcium and iron follow the pattern previously described for the open area scale while zinc appears to be

present mainly in the iron-rich areas. For the whole external surface of this cross-section, the oxide layer immediate to the base alloy, of about 10 μm, was enriched in iron.

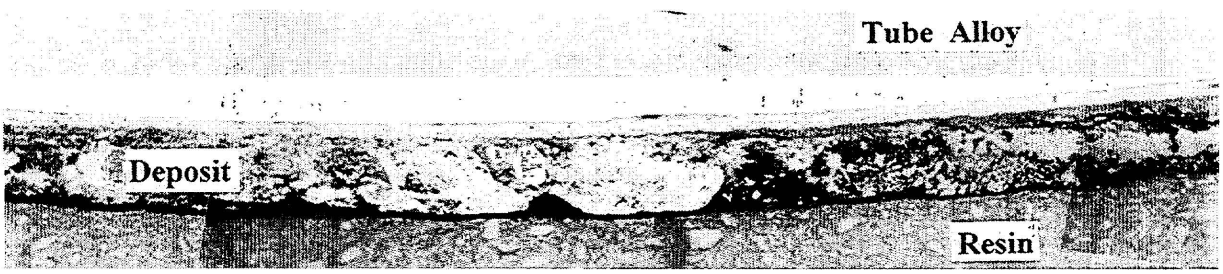


Figure 11: Cross-section of the deposit immediately over the sludge pile (120X)

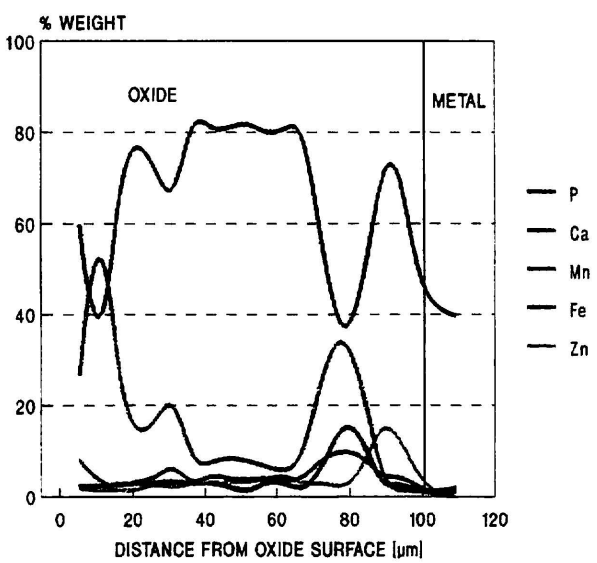


Figure 12: Concentration profiles from the scale over the sludge pile. Zone 1.

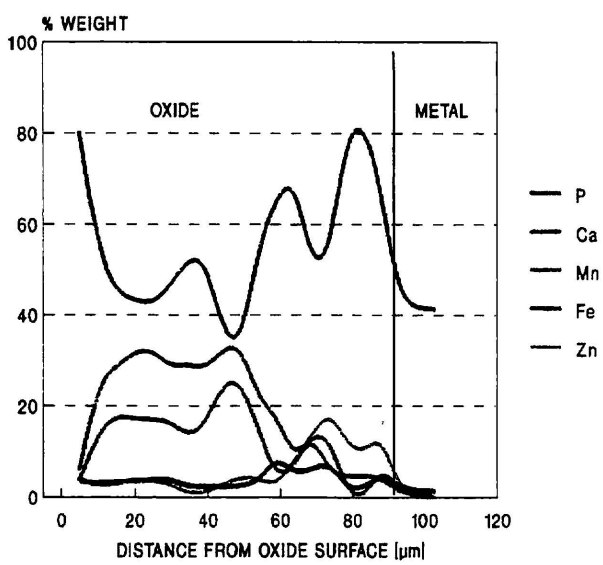


Figure 13: Concentration profiles from the scale over the sludge pile. Zone 2.

Spalling of the deposit was observed in different zones of the outer surface. The metallographical examinations showed that a thin layer of iron-rich oxide of about 2 μm remained on the tube surface. Nickel and chromium due to the base metal were also identified. No evidence of base metal attack was found.

4.3. Chemical composition and morphology of sludge samples

Samples of the deposits were taken at the first tube support plate and at the top, medium height and bottom of the 15 cm sludge pile at the tubesheet/sludge interface. Chips of the samples were examined using SEM/EDS. The rest of the samples was dissolved with *aqua regia* and chemically analized. The bulk composition obtained by the chemical procedure followed a similar trend to the composition yielded by the surface analytical technique (EDS). The major elemental constituent of all samples was iron, owing to the corrosion of the carbon steel feedtrain piping. Using either technique, the amount of iron increased from the sample at the tube support plate down to the sample over the tubesheet/sludge interface. The relative bulk concentration of iron ranges from around 35% at the tube support plate to over 50% at the bottom. Significant concentrations of species resulting from brass condenser corrosion and cooling water in-leakage, such as copper, zinc, calcium, magnesium, manganese, silicon and aluminum were also found. Calcium was the predominant element after iron and the bulk copper content was always less than 10%.

Analysis by SEM/EDS reflects the heterogenous nature of the morphology and composition of the samples that vary both in-depth and over the surface of each sample. Agglomerates of iron rich crystallites (95%), ranging in size from 1 to 15 μm, were observed next to regions with large crystalline particles of different size, shape and composition. The morphological observations indicated clusters of larger, well-shaped crystals from the mid-height to the bottom of the sludge pile.

4.4. Discussion

The morphology and composition of the oxide film found on the inner surface of the tube reflect not only the corrosion process of the base material but also the interaction with the primary coolant that results in growth of crystals and deposition of corrosion products. On account of both these processes, the thickness of the film along the length of the tube varies, as is shown in Figure 8, related with variables such as the concentration of iron in the coolant and the solubility of magnetite, temperature, local water chemistry, etc. The thicknesses measured at different locations of the tube and the iron enrichment at the oxide/coolant interface are in agreement with the oxide layers found in the corrosion test samples from the hot leg autoclaves.

Analysis of the scale on the outer surface of the tube shows the contribution of corrosion products from the feedtrain components and impurities due to in-leakage of lake water. Iron, as expected, is the major component of the film but calcium, zinc, phosphorous and manganese are also present. As is shown in the concentration profiles from the open area, see Figure 9, the salts with inverse temperature solubility, such as those formed by calcium, will precipitate close to the base alloy

interface where boiling is occurring. The same elements form the 100-μm scale deposited on the tube over the sludge pile where, although iron is still the main component, the contribution of the other elements to the scale is significant and their distribution pattern is heterogenous. This is also the case for the samples of the deposits at the first support plate and the sludge pile. The presence of larger crystals predominating from the mid-height to the bottom of the sludge pile is in accordance with the precipitation and recrystallization processes due to boiling at this region, close to the tubesheet, under the deposits.

5. CONCLUSIONS

- The different behaviour of the Alloy 800 corrosion test samples exposed at inlet and outlet SG conditions is clearly related to the degree of saturation in corrosion products of the coolant. The level of corrosion products in the overflowing solution has a strong influence on the thickness and the structure of the oxide film formed on Alloy 800 in lithiated high temperature water. Thus, even allowing for such differences as flow rate and heat transfer conditions, primary side fouling of SG tubing is likely to occur.

- In agreement with the results and assumptions from the corrosion monitoring programme, the morphology and the thickness of the oxide found in the primary side surface of the hot leg section of a SG tubing removed from the Embalse NPP showed that growth of crystals by precipitation and deposition of corrosion products take place to a large extent.

- Significant deposition of corrosion products was found on the secondary side surface of the tube, which exhibited an oxide scale layer ranging from 30 μm in the open area to 100 μm over the top of the sludge pile. The main constituents of the deposits are feedtrain corrosion products and species resulting from in-leakage of cooling water.

- The deposits at the tube support plate and the sludge samples consisted mainly of iron but a significant concentration of species resulting from the condenser corrosion and lake water in-leakage was found.

6. REFERENCES

1. Dow B.L., Thomas R.C., "SG status: worldwide statistics reviewed", Nuclear Engineering International 40 (1995) 18.
2. Stipan L.M., Tapping R.L., " Tube plugging: looking behind the trends", Nuclear Engineering International 40 (1995) 19.

3. Burrill K.A., Turner C.W., "Control of reactor inlet header temperature (RIHT) rise in CANDU", Proc. of Second Int. Steam Generator and Heat Exchanger Conference, Session #7, Toronto, Canada, p. 7.125, 1994.
4. Villegas M., Olmedo A.M., Bordoni R., Alvarez M.G., Miyagusuku M., Saínz R., "Surveillance program of corrosion-related degradation of structural materials in primary reactor coolant", IAEA Specialists Meeting on the Effectiveness of Methods for the Detection and Monitoring of Age Related Degradation in Nuclear Power Plants, Session #1, Bariloche, Argentina, 1995.
5. Fernandez A., Fiorini R., Rosales H., Saínz R., Yacobone W., Blesa M.A., Bordoni R., Chocrón M., Geldstein M.C., Helzel García L.J., Maroto A.J.G., Miyagusuku M., Olmedo A.M., Piacquadío N.H., Urrutia G.A. and Villegas M., "The effect of mixed-bed resin ingress into Embalse PHTS", Proc. of The Exchange Operational Safety Experience of Pressurized Heavy Water Reactors", IAEA/COG, Session #3, Embalse, Argentina, 1991.
6. Mann G.M.W., Proc. Int. Congress in "High Temperature High Pressure Electrochemistry in Aqueous Solutions", NACE-4, 1976, p. 34.
7. Tapping R.L., Davidson R.D., McAlpine E., Lister D.H., "The composition and morphology of oxide films formed on type 304 SS in lithiated high temperature water", Corros. Sci. 26 (1986) 563.
8. Alvarez M.G., Olmedo A.M., Villegas M., "Corrosion behaviour of Alloy 800 in high temperature aqueous solutions: long term autoclave studies", Journal of Nuclear Materials 229 (1996) 93.
9. Olmedo A.M., Villegas M., Blesa M.A., Fernández Prini R., Maroto A.J.G., "Corrosion of austenitic stainless steels in water at 220°C", Proc. VII Interamerican Conf. on Materials Technology, Mexico, 1981, p. 27.
10. Taylor G.F.,"Corrosion monitoring in CANDU nuclear generating stations", Proc.of CORROSION/77 (NACE), San Francisco, California, 1977, paper 119.
11. Schuster E., Neeb K.H., Ahlfanger W., Henkelman R., Jarnstromm R.T., "Analyses of primary side oxide layers on steam generators tubes from PWR's and radiochemical issues on the contamination of primary circuits", Journal of Nuclear Materials 152 (1988) 1.

DISCUSSION

Authors: A.J.G. Maroto, M.A.Blesa, M. Villegas, A.M. Olmedo, R. Bordoni, M.G. Alvarez, R. Sainz, Comisión Nacional de Energía Atómica, and Central Nuclear Embalse, Nucleoeléctrica Argentina

Paper: Corrosion of Alloy 800 in PHWR Primary and Secondary Conditions

Questioner: J. Nickerson, AECL

Question/Comment:

What was the sludge pile indicated from the pulled tube? And does the plant have any plan to remove the sludge pile?

Response:

The sludge pile was 15 cm deep when the tube was removed. I am not aware of future plans of the plant concerning the removal of the sludge pile.

Questioner: M. Brett, Ontario Hydro

Question/Comment:

Did you find Pb in the secondary side deposits of the pulled SG tube?

Response:

No, Pb was not detected either in the deposits on the outer surface of the tube or in the samples taken from the first tube support plate and the sludge pile.